JOURNAL OF CATALYSIS 143, 369–380 (1993)

Radioactive Tracer Techniques for Study of Reactions on Industrial Catalysts

I. Kinetics of the Enhanced Desorption of Carbon Monoxide Due to the Influence of Carbon Monoxide in the Gas Phase

ULF SCHRÖDER[1] AND NILS-HERMAN SCHÖÖN

Department of Chemical Reaction Engineering, Chalmers University of Technology, S-412 96 Gothenburg, Sweden

Received September 30, 1992; revised May 11, 1993

An *in situ* radioactive method for studying adsorption-desorption dynamics has been used to determine the kinetics of the enhanced desorption of CO from a commercial Pd/Al_2O_3 catalyst at 50 Pa $\leq P_{CO} \leq$ 200 Pa and 233 K $\leq T \leq$ 333 K. The enhanced desorption was found to be much slower than at vacuum conditions reported in the literature. This desorption was found to be first-order with respect to both the partial pressure of CO and the fractional coverage of labelled CO. The quantitative evaluation of the rate constant required a determination of the external and internal mass transport steps and the linear absorption coefficient of the radioactivity.

INTRODUCTION

Radioactive tracer techniques have long been used to study the kinetics and mechanism of chemical reactions. These techniques have also been used successfully in the study of reactions proceeding in the presence of a solid catalyst. Comprehensive reviews of this application have been given by Campbell and Thomson (*1*), Berndt (*2*), and Thomson (*3*), among others.

In order to obtain a deeper knowledge of the processes occurring on the surface of the solid catalyst, it is of vital interest to monitor the processes directly. The radioactive techniques have hereby been a valuable complement to the different spectroscopic methods. A long-felt need is to be able to study chemical surface processes at elevated pressure and in the presence of a working supported catalyst, instead of in the presence of a single metal crystal at high vacuum. This need has limited the number of spectroscopic methods in these studies and calls for further attention to radioactive tracer techniques.

Direct observations of the surface processes on supported catalysts at industrial reaction conditions are difficult because of the limited durability of the measuring equipment for radioactivity at elevated temperature. Moreover, the most often used isotopes for labelling (^{14}C, ^{35}S, ^{3}H) are soft β^- emitters. The self-absorption of this radiation in the catalyst disc, together with a slow pore diffusion, has minimized the use of radioactive tracer techniques for direct observation of surface processes on supported catalysts. However, the low energy of these soft β^- emitters is an advantage since safe handling of such tracers is easily accomplished.

In this work, a radioactive technique has been used to study the kinetics of the isotopic exchange between CO in the gas phase and CO adsorbed on an industrial Pd/Al_2O_3 catalyst at atmospheric conditions. The radioactive technique is based on the use of

[1] To whom correspondence should be addressed.

0021-9517/93 $5.00

a gas flow cell where one window consists of a solid scintillator. The scintillator is connected to a photomultiplier via an external cooled light conductor in order to decrease the risk of overheating the counter. Self-absorption of the radiation and the slow pore diffusion have been corrected for based on separate determinations of the self-absorption coefficient and the effective diffusivity. The gas flow cell is, moreover, an open reactor with continuous gas flow, which minimizes the radioactivity of the gas phase in the cell.

Investigations of the isotopic exchange between adsorbed CO and gas-phase CO are an important part of mechanistic studies of the Fischer–Tropsch process and the methanol synthesis in order to learn whether a dissociation of CO is an initial step in these processes. These studies demand that two different carbon isotopes, as well as two oxygen isotopes, are used. A somewhat independent observation is that the very slow thermal desorption of CO from a metallic catalyst surface is dramatically enhanced when CO is added to the gas phase. This enhanced desorption is found both in vacuum and in the presence of an inert gas at room temperature. The desorption is not preceded by any dissociation and recombination of CO on the surface but occurs via the displacement of an adsorbed CO molecule as a whole.

Klier *et al.* (*4*) were the first to report this enhanced desorption of CO by studying the desorption of CO from (100) and (110) Ni crystal faces at low pressure using ^{14}CO. This influence of gas-phase CO on the CO desorption soon became the object of a great number of studies during the 1970s and 1980s (*5–25*). All these studies were performed at high vacuum conditions with unsupported polycrystalline metals or single crystal surfaces of metals as catalysts. Kinetic aspects of this exchange were, however, the object of rather few studies (*4, 9–12, 25*). It has been shown recently that the desorption of CO can also be enhanced by the presence of compounds other than CO in the gas phase (*16, 26–31*). The enhanced desorption of CO is also observed at reaction conditions found in industrial processes (*32–35*). These observations initiated the present study to determine the kinetics of the isotopic exchange between gas-phase CO and adsorbed CO at conditions more related to technical reality.

EXPERIMENTAL

Reactor and Detector

Figure 1 shows a cross section of the reactor, which has been described in detail elsewhere (*36*). The reactor cell is the same as the one used for *in situ* transmission FTIR studies (*37*). However, one of the windows is replaced by a europium-doped CaF_2 window. This acts as a scintillator, which transmits light when β^- particles from the radioactive decay are absorbed. The light is transmitted to a photomultiplier, via a cooled glass rod to prevent overheating of the photomultiplier. The signal from the photomultiplier is preamplified and analyzed by a rate-meter. The reactor can be heated by cartridge heaters in the flanges, and the experiments at temperatures below 25°C were made with the reactor immersed in a refrigerant.

A 5 wt% Pd/Al_2O_3 catalyst (Aldrich, catalogue no. 20,571-0) with a particle size of less than 44 μm was used in all experiments. About 0.15 g of the catalyst powder was pressed under 7 tons of pressure into a disc and placed in the reactor. This preparation of the disc followed the common procedure used in FTIR studies (*38*). Before the experiments the catalyst disc was treated with H_2 at 100°C for 1 hr. The percentage exposed of Pd (Pd dispersion) in the catalyst was determined by CO adsorption assuming the stoichiometry CO/Pd = 1. This determination was performed with the catalyst disc mounted in the reactor after treatment with H_2.

The gases used (Ar, H_2, CO) were all with a purity better than 99.98% and were delivered by AGA (Sweden).

In the labelling procedure, 5 mCi ^{14}CO (53

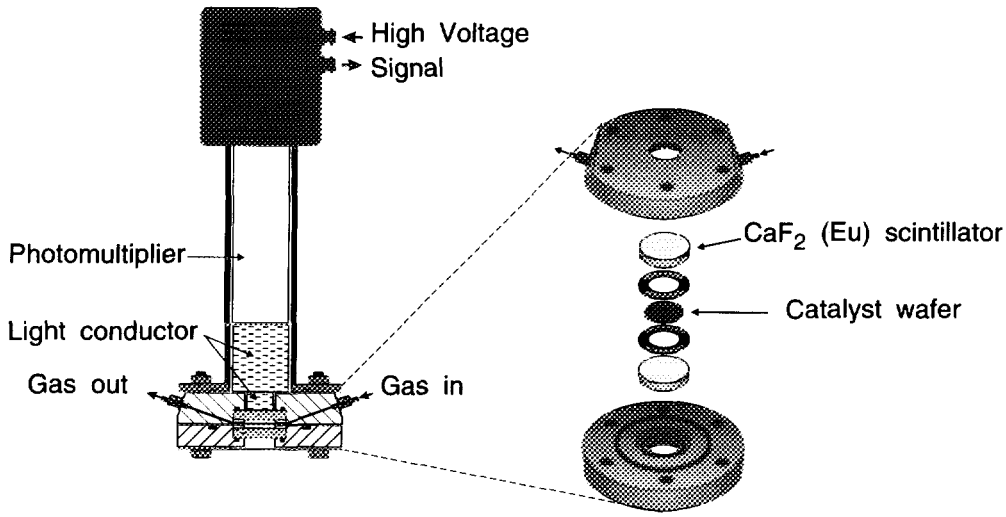

FIG. 1. The reactor for *in situ* radioactive tracer experiments.

mCi $mmol^{-1}$) Amersham (England), delivered in a glass ampoule, was transferred to a 1-liter evacuated gas flask. This was then filled to 35 atm with 5700 ppm CO in Ar. The labelled CO resultant concentration was 5775 ppm. Mixtures with lower concentration of labelled CO were obtained by dilution with Ar.

Some Material Data and Physical Parameters

To evaluate the kinetic parameters for the desorption, the following must be considered:

—mixing characteristics in the cell;
—mass transfer between the gas bulk and the disc;
—mass transport in the catalyst disc;
—absorption of β^- particles in the catalyst disc.

The bulk flow through the cell was studied in pulse-response experiments in a scaled-up Plexiglas reactor, and also by computer simulations of the flow in the original cell. These studies showed that the flow was divided into parallel laminar flow branches with different residence times. The bulk flow studies thus showed that the flow conditions in the cell are very complex. A mathematical description of the flow will require a comprehensive study which may not be necessary for the evaluation of the kinetic properties of the isotopic exchange. The flow was approximated as ideal plug flow in the determinations of the external mass transfer coefficient and the effective diffusivity. In the isotopic exchange studies the cell was considered as a differential cell, since the time constant for the exchange process was much greater than the residence time of the gas flow in the cell.

The effective diffusivity of CO in the catalyst was obtained by the Wicke–Kallenbach method (*39*). A catalyst disc was pressed and placed in a special Plexiglas cell. Pure Ar flowed over one side of the catalyst disc, while 112 ppm CO in Ar flowed over the other side. Measuring the CO concentration in the outflow gave the diffusion rate. The measurement was performed at 25°C. Since the pore diffusion should proceed at Knudsen regime conditions (cf. data in Table 1), the diffusivity at other temperatures is calculated from the square-root dependence on the absolute temperature.

TABLE 1

Catalyst Disc Properties

Pd content	5 wt%
Pd dispersion	0.13
BET area	118 $m^2 g^{-1}$
Average pore radius	75 Å
Catalyst disc porosity, ε	0.59
Catalyst disc density, ρ	1506 kg m^{-3}
Disc thickness	0.23 mm
Disc diameter	18 mm
Mass transfer coefficient for CO, k_c (25°C)	6.3×10^{-3} m s^{-1}
Effective diffusivity for CO in the disc, D_{eff} (25°C)	1.2×10^{-6} m^2 s^{-1}
Absorption coefficient for β^--particles in the catalyst, μ	12,389 m^{-1}

The external mass transfer coefficient for CO was measured indirectly. A disc of naphthalene was placed in the reactor cell, and the rate of vaporization of naphthalene was measured at different flow rates at 25°C. The saturation concentration was obtained by passing the outflow gas through a tube filled with an excess of naphthalene powder. An FID detector was used to measure the concentrations. A material balance over the reactor assuming ideal plug flow gave the mass transfer coefficient for naphthalene. The mass transfer coefficient for CO was obtained by multiplication with the ratio of the diffusivities of CO and naphthalene. The ratio value used in the calculation was equal to 3.6 at 25°C. The mass transfer coefficient at other temperatures was obtained by the empirical correlation $k_c \propto T^{1.75}$ (*40*).

The linear absorption coefficient for the β^- particles in the catalyst was measured as follows. A catalyst disc of a known thickness was placed between the detector and a radioactive labelled catalyst disc. The coefficient was calculated from the decrease in the observed radioactivity, assuming an exponential decrease in the β^--particle flux through the catalyst disc. The value of the linear adsorption coefficient (Table 1) indicates that only about 24% of the β^- particles emitted from the middle of the disc reached the surface of the disc.

THEORY

The adsorption and desorption rates of CO are measured at steady-state conditions in this study. This means that the total adsorption rate is equal to the total desorption rate. Moreover, the total fractional coverage and concentration of CO are constant. A step from labelled to unlabelled CO in the feed gas will thus change only the ratio between the labelled and the unlabelled CO in the gas phase and on the catalyst surface.

The total desorption rate of CO can be written as

$$r_{d,tot} = k_d P^n_{CO,tot} \theta_{CO,tot}. \quad (1)$$

The palladium part of the catalyst is considered to be completely covered with CO at the relatively high partial pressure of CO used in this study. The total fractional coverage of CO in Eq. (1) is normalized to unity, i.e., $\theta_{CO,tot} = 1$, despite the fact that the maximum fractional coverage according to the number of exposed palladium atoms is less than unity (*41*).

Normally it is supposed that the desorption rate is independent of the partial pressure, i.e., $n = 0$. With n equal to zero, the expression for the ordinary thermal desorption is obtained. However, as is shown, n is not equal to zero when CO is present in the gas phase.

The desorption rate of labelled CO can be written as

$$r_d = \frac{\theta}{\theta_{CO,tot}} r_{d,tot}, \quad (2)$$

where θ is the fractional coverage of labelled CO. In the same way, the adsorption rate of labelled CO is expressed as

$$r_a = \frac{P_{CO}}{P_{CO,tot}} r_{a,tot} = \frac{P_{CO}}{P_{CO,tot}} r_{d,tot}, \quad (3)$$

where P_{CO} is the partial pressure of labelled CO. Since isotopic effects can be neglected, ^{14}CO can be considered to be chemically and physically indistinguishable (other than the radioactivity) in the labelled CO. During the isotopic exchange process, the labelled

CO is diluted with unlabelled CO of the same partial pressure. When the undiluted labelled mixture is in equilibrium with the catalyst, the fractional coverage of labelled CO is given the value $\theta = 1$. Correspondingly the partial pressure of labelled CO in the fresh labelled gas mixture is $P_{CO} = P_{CO,tot}$.

The local change in the labelled CO coverage can, therefore, be written as

$$\frac{\partial \theta}{\partial t} = \frac{1}{N_s \rho}(r_a - r_d), \tag{4}$$

where N_s is the molar site density of the uniformly distributed active sites per mass of the catalyst and ρ is the density of the catalyst. The parameters that have to be determined are the rate constant, k_d, and the reaction order, n.

A mathematical model is needed in order to evaluate the kinetic parameters. The model must describe how the fractional coverage and concentration of labelled CO change with time and position in the catalyst disc. Furthermore, it must describe how the observed radioactivity depends on the fractional coverage of the labelled CO. This requires us to account for the absorption of β^- particles in the catalyst.

A mass balance in the gas phase, inside the catalyst pores, describes how the concentration of labelled CO changes with time and position,

$$\varepsilon \frac{\partial C}{\partial t} = D_{eff} \frac{\partial^2 C}{\partial x^2} + (r_d - r_a), \tag{5}$$

where D_{eff} is the effective diffusivity, C is the local concentration of labelled CO, ε is the void fraction of the catalyst, and x is the length coordinate orthogonal to the external surface of the catalyst disc.

The initial conditions, for the experiment where a step from labelled to unlabelled CO is made, become

$$\theta(0, x) = 1 \tag{6}$$

$$C(0, x) = P_{CO,tot}/RT. \tag{7}$$

The boundary condition in the center of the disc, $x = L/2$, is

$$\frac{\partial C(t, L/2)}{\partial x} = 0. \tag{8}$$

To obtain the boundary condition at the external surface, a mass balance over the reactor is needed. The reactor is treated as a differential one, since the residence time is very short compared to the time for the desorption and the adsorption. The material balance becomes

$$q(C_f - C_b) = V \frac{\partial C_b}{\partial t} - D_{eff} A \frac{\partial C(t, 0)}{\partial x}, \tag{9}$$

where q is the volumetric flow rate, A the external catalyst disc area, C_f the inlet concentration, and C_b the bulk concentration of the labelled CO. The accumulation in the gas phase, $V(\partial C_b/\partial t)$, is neglected since the accumulation on the catalyst surface is much greater. The flux of labelled CO from the external surface of the catalyst disc to the bulk gas is given by

$$N = k_c(C(t, 0) - C_b). \tag{10}$$

This flux can also be written as

$$N = D_{eff} \frac{\partial C(t, 0)}{\partial x}. \tag{11}$$

Combining Eqs. (9)–(11) and neglecting the gas-phase accumulation gives

$$C(t, 0) = C_f + \left(\frac{1}{k_c} + \frac{A}{q}\right) D_{eff} \frac{\partial C(t, 0)}{\partial x}, \tag{12}$$

where $C_f = 0$ with a step from labelled to unlabelled CO.

Equation (5) was discretized in the spatial direction using orthogonal collocation, and the resulting ordinary differential equation system was solved for different values of n and k_d using a semiimplicit Runge–Kutta method. Eqs. (3) and (4), with the boundary and initial conditions, give the local coverage of labelled CO.

The next step is to express the observed radioactivity as a function of the local coverage. The contribution of the emitted β^- particles from the disc element dx, at the posi-

tion x, to the observed radioactivity can be written as

$$dI = k\,\theta(x, t)\exp(-\mu x)\,dx, \qquad (13)$$

where μ is the linear absorption coefficient for the β^--particles in the catalyst and k is a constant. The local coverage is symmetric about the center line $x = L/2$, since the gas is flowing on both sides of the catalyst disc. Therefore, it is sufficient to integrate from the external surface to the middle of the disc to obtain the total calculated radioactivity giving

$$I(t) = \int_0^{L/2} k\,\theta(x, t)\,[\exp(-\mu x) + \exp(-\mu(L - x))]\,dx. \qquad (14)$$

The term $\exp(-\mu(L - x))$ gives the contribution from that half of the disc which is farthest away from the scintillator.

When the catalyst disc is in isotopic equilibrium with the fresh labelled gas mixture, the local coverage is $\theta(x, t) = \theta_{CO,tot} = 1$, and the observed activity is I_{max}. This makes it possible to calculate k from Eq. (14), giving

$$k = \frac{\mu I_{max}}{1 - \exp(-\mu L)}. \qquad (15)$$

The relative radioactivity $I(t)/I_{max}$ was calculated for different values of n and k_d in order to find the values giving the best agreement with the measured relative count rate. The relative count rate was defined as the ratio between the count rate at the time t and the maximum count rate at isotopic equilibrium with the undiluted labelled gas mixture.

RESULTS AND DISCUSSION

Enhanced Desorption of CO at High Fractional Coverage of CO

The thermal desorption of labelled CO is very slow at 20°C as indicated by the constant radioactivity of the catalyst disc (Fig. 2). This agrees with the well-known high adsorption energy of CO on Pd. The low decrease of radioactivity also ensures that a reaction between adsorbed CO and remaining small amounts of H_2O if any in the porous catalyst does not influence the interpretation of the result. This reaction has been shown to result in the desorption of significant amounts of CO as CO_2 during TPD (*42, 43*). However, in the presence of CO in the gas phase, the radioactivity of the catalyst disc decreases very rapidly (Fig. 2). This shows that the adsorbed CO is displaced rapidly by CO in the gas phase. Such enhanced desorption has been demonstrated by many authors at vacuum conditions with unsupported polycrystalline metal surfaces or with single-crystal surfaces. In these experiments the metal surfaces were only partly covered with CO. In the present study, however, the fractional coverage of CO is constant and at maximum throughout all the experiments. This fact is important in looking for the mechanism of the isotopic exchange at high fractional coverage, as discussed further below.

Influence of CO Pressure on the Enhanced Desorption

The desorption rate of CO is dependent not only on the temperature but also on the CO pressure (Fig. 2). The desorption rate of labelled CO was described as a first-order process with respect to both the partial pressure of CO and the fractional coverage of labelled CO. A regression analysis with respect to the reaction order in the partial pressure of CO gave the value 0.9, but since the minimum of the residual sum of squares was shallow, the value 1.0 was chosen, based on the assumption that a first-order process may be more reasonable to accept from a mechanistic point of view.

In these experiments the partial pressure was $50\ \text{Pa} \le P_{CO} \le 200\ \text{Pa}$. The rate constant was determined to be $k_d = 0.018$ mol $m^{-3}(cat)s^{-1}\ Pa^{-1}$ at 20°C. Figure 3 shows that the sum of squares of residuals reaches a distinct minimum at this value. The sum of squares function is, however, asymmetric with respect to the minimum. This is explained by the fact that the mass transport

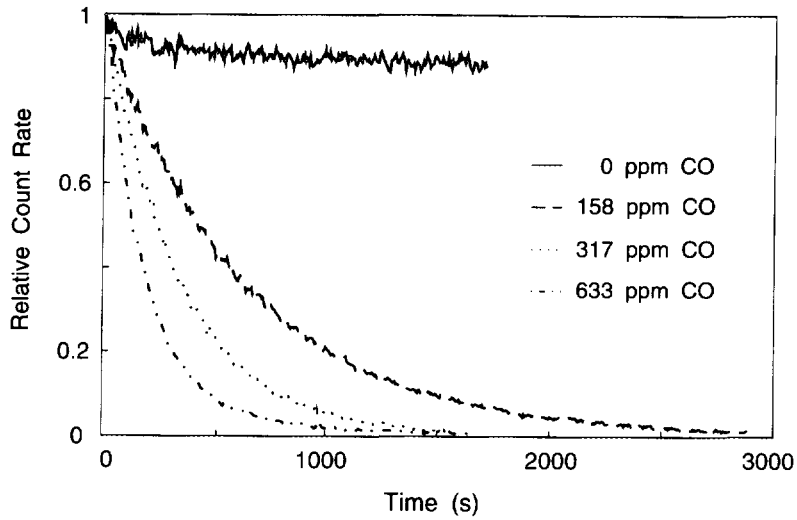

FIG. 2. Effect of CO pressure on the desorption rate of preadsorbed labelled CO on a 5 wt% Pd/Al_2O_3 catalyst: $T = 298$ K, $P = 10^5$ Pa, and $q = 3 \times 10^{-6}$ m^3 s^{-1}; inert gas, argon.

resistance becomes dominating at higher values of k_d. From the experimentally determined values of the rate constants for the external and internal mass transport (Table 1), it is possible to decide whether the rate constant of the desorption can be determined or not. For k_d values above 0.15 mol m^{-3}(cat) s^{-1} Pa^{-1} the desorption at 20°C is essentially dependent only on the mass transport.

As also shown by Fig. 4, where a step from unlabelled to labelled CO is made, the observed relative count rate agrees well, without any systematic or periodic deviation, with the relative radioactivity $I(t)/I_{max}$. This shows that the rate equation is acceptable from a statistical point of view. The relative count rate is unity when the labelled CO is maximum and homogeneously adsorbed throughout the whole catalyst disc.

Influence of Temperature on the Enhanced Desorption

Desorption experiments were performed at 233 K $\leq T \leq$ 333 K and at 95 Pa CO partial pressure. From an Arrhenius plot (Fig. 5), the preexponential factor and the activation energy were found to be $k_d^0 = 0.116$ mol m^{-3}(cat) s^{-1} Pa^{-1} and $E_a = 4.6$ kJ mol^{-1}, respectively. This preexponential factor value corresponds to $k_d^0 = 1.26 \times 10^{-3}$ s^{-1} Pa^{-1}, since the number of adsorption sites is 92 mol m^{-3}(cat) (cf. Table 1). The values of k_d^0 and E_a can be compared with those given by Yamada *et al.* (*12*) obtained at 339 K $\leq T \leq$ 466 K and 1.3×10^{-6} Pa $\leq P_{CO} \leq 1.3 \times 10^{-5}$ Pa on unsupported polycrystalline Pd. They reported $k_d^0 = 2.5 \times 10^6$ s^{-1} Pa^{-1} and $E_a = 20.5$ kJ mol^{-1}. Moreover, the process was found to be 0.79 order in the CO pressure. If their values obtained at vacuum conditions are extrapolated using the conditions of the current study, a nine to ten order-of-magnitude higher desorption rate than that obtained in the current study would be expected. Such a rapid desorption is impossible to analyze kinetically with the present technique, since the diffusional transport steps are too slow. A comparison of the maximum transport rates based on the data in Table 1 with the observed desorption rate showed that the transport steps are not limiting in the present study. However, if the mass transport constants for the external transport and the effective diffusivity of the pore transport are overestimated by a factor

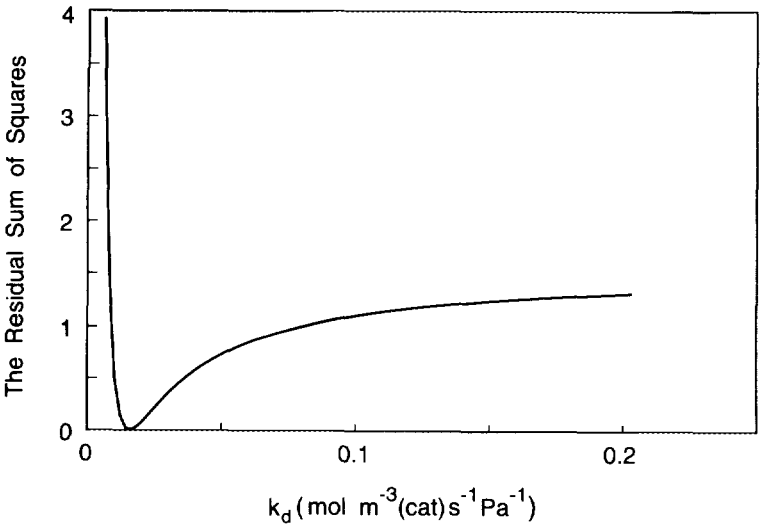

FIG. 3. The residual sum of squares as a function of the rate constant for the desorption. k_d is defined according to $r_d = k_d P_{CO,tot} \theta$: $T = 293$ K, 950 ppm CO in Ar, $P = 10^5$ Pa, and $q = 3 \times 10^{-6}$ m^3 s^{-1}.

of about five, the rate constant of the desorption cannot be determined at room temperature. A common way to decrease the influence of the transport steps is to make use of the low activation energy for these steps and thus perform the experiments at low temperature. Since the enhanced desorption has a low activation energy, demonstrated by Yamada *et al.* (*12*), Malakhov *et al.* (*5*), and by the present study, this approach cannot be used.

Apart from Yamada *et al.* (*12*), Matsushima (*9–11*), Klier *et al.* (*4*), and Guo *et al.* (*25*) have also quantitatively analyzed

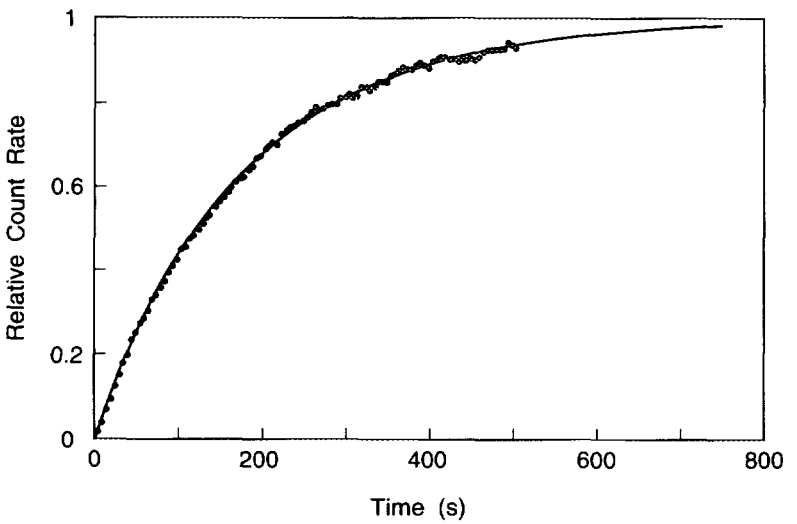

FIG. 4. The change in the observed and calculated relative count rate for a step from unlabelled to labelled CO: $T = 293$ K, 950 ppm CO in Ar, $P = 10^5$ Pa, and $q = 3 \times 10^{-6}$ m^3 s^{-1}. (·····) Relative count rate, observed; (_____) calculated relative radioactivity $I(t)/I_{max}$ from the mathematical model.

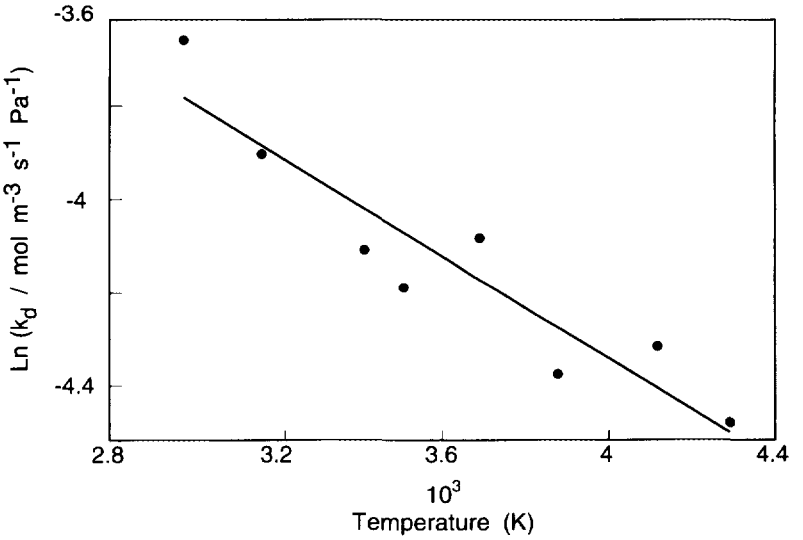

FIG. 5. The rate constant as a function of temperature for the desorption of CO from a 5 wt% Pd/Al_2O_3 catalyst: 950 ppm CO in Ar, $P = 10^5$ Pa, and $q = 3 \times 10^{-6}$ m^3 s^{-1}. (·····) k_d Value calculated on the basis of experiments and the mathematical model Eqs. (1)–(15) with $n = 1$; (_____) regression line.

the kinetics of the enhanced desorption of CO at low pressures. These investigations showed further that the isotopic exchange is a rapid process.

Some Explanations for the Enhanced Desorption of CO

It is an unanimous opinion that the enhanced desorption of CO occurs via the displacement of an adsorbed CO molecule as a whole rather than via a dissociation–recombination elementary process. The enhanced desorption of CO has hitherto been explained by some different mechanisms. Yates and Goodman (*8*) investigated how the thermal desorption states of CO on Ni(100) were influenced by the presence of a high flux of CO at 250 K and at low pressure. They found that preadsorbed $^{12}C^{18}O$ in the β_2 state was redistributed over all the desorption states by the CO flux. The desorption energies of the states were also found to decrease at high CO flux. Their explanation of the fast displacement by CO in the gas phase at low temperature is that all CO is desorbed from the α states. A similar explanation was given by Klier *et al.* (*4*) for the rapid isotopic exchange between adsorbed CO on Ni(110) and Ni(100) and CO in the gas phase. They interpreted this result as indicating a considerable degree of translational freedom in the adsorbate. This lateral interaction model gives, however, only a qualitative explanation.

A theoretical study by Lombardo and Bell (*24*) based on Monte Carlo simulations supports the opinion that the enhanced desorption of CO at vacuum conditions may be a direct consequence of the somewhat increased coverage of CO caused by the CO flux into the vacuum chamber. The increased coverage was shown to give a pronounced decrease of the average activation energy of desorption at a fractional coverage of about 0.8. These simulations would thus indicate that the enhanced desorption found experimentally is not a new phenomenon but may partly be ascribed to the choice of experimental conditions and to the fashion of treating the data.

An alternative explanation may be based on the observations made by Yates *et al.*

(6) in a study of the CO desorption from isolated Rh sites. They suggested, on the basis of a FTIR study, that the isotopic exchange of CO may proceed through the formation of the intermediate $Rh(CO)_3$. If this kind of intermediate can be formed also in the isotopic exchange on Pd, the influence of the CO pressure and the fractional coverage of labelled CO on the desorption rate according to Eqs. (1) and (2) is then easy to explain. The same influence would occur if the reactants of the adsorption-desorption process instead pass through a transition state as proposed in the SN2 mechanism well-known from the literature of organic chemistry. This mechanism was discussed in connection with adsorption-desorption displacement processes by Ertl (*44*).

The mechanisms including the formation of an intermediate or a transition state do not, however, account for the great difference of the rate constant value between low and high fractional coverages of CO. This great difference indicates that the mechanism is more complicated.

It should be recalled that the rate constant was calculated with the assumption that the fractional coverage of CO is maximal already at the lowest CO pressure and does not increase at increasing CO pressure. The influence of the CO pressure on the exchange rate may therefore be explained by a direct interaction between gas-phase CO and adsorbed CO. If, however, the fractional coverage of CO is only close to maximum at the lowest CO pressure, then it is possible to obtain an increased coverage of CO by increasing the CO pressure. This situation is supported by the fact that a small amount of adsorbed CO was easily desorbed when the gas phase contained only Ar (cf. Fig. 2). It is therefore reasonable to think that a common thermal adsorption–desorption process occurs in the presence of CO in the gas phase via a small fraction of vacant active sites.

The proportionality between the exchange rate and the CO pressure found in the present study may be explained by a model similar to the one proposed by Lombardo and Bell (*24*). Their model assumes adsorption with different adsorption energies, which are in equilibrium due to surface diffusion. The exchange process will therefore mainly proceed through states with low desorption energies. The enhanced desorption rate and its pressure dependence is explained by an increase in fractional coverage at higher CO pressure. The lower value of the rate constant found in the present study, compared to the one reported by Yamada *et al.* (*12*) at low CO coverage, may be explained by the lower surface mobility of CO at the high coverage. This means that the different states are no longer in equilibrium, and the rate-determining step is a restricted surface diffusion instead of thermal desorption. The low activation energy may support a slow surface diffusion step or a direct exchange process. However, if the surface diffusion is the rate-determining step, the exchange rate would not be expected to increase proportionally with the CO pressure.

CONCLUSIONS

The present study showed that the radioactive tracer technique is well suited to monitor rapid changes of the radioactive labelled compounds adsorbed on a thin disc of a porous catalyst. The time constant of the solid scintillator and the electronic equipment was much less than the time constant of the exchange processes.

The exchange between preadsorbed CO on a supported commercial Pd catalyst and gas-phase CO at 50 Pa $\leq P_{CO} \leq$ 200 Pa was found to be very rapid, despite the well-known slow thermal desorption of CO in vacuum or in the presence of an inert gas. This result indicates that the CO exchange may be very rapid in heterogeneous catalytic industrial processes with CO present in the gas phase.

Despite the low fraction of vacant sites, it seems possible that the same mechanism may explain the exchange process as given by Lombardo and Bell (*24*) for this exchange

at low fractional coverage. It cannot, however, be excluded that the exchange proceeds via a direct interaction between adsorbed CO and gas-phase CO.

APPENDIX: NOTATION

A	area of catalyst disc, m^2
C	concentration of labelled CO in the gas phase of the catalyst, mol m^{-3}
C_b	concentration of labelled CO in the bulk gas phase, mol m^{-3}
C_f	concentration of labelled CO in the feed, mol m^{-3}
D_{eff}	effective diffusivity of CO in porous catalyst disc, m^2 s^{-1}
E_a	activation energy of enhanced desorption, kJ mol^{-1}
I	measured radioactivity, cps
I_{max}	maximum measured radioactivity, cps
k	proportionality constant between the local fractional coverage of labelled CO and the local radioactivity
k_c	mass transfer coefficient, m s^{-1}
k_d	desorption rate constant, mol m^{-3} (cat)s^{-1} Pa^{-n}
k_d^0	preexponential factor of k_d, mol m^{-3} (cat)s^{-1} Pa^{-n}
L	thickness of the catalyst disc, m
n	reaction order with respect to CO pressure
N	the flux of labelled CO from the external surface, mol s^{-1} m^{-2}
N_s	site density, mol (kg catalyst)$^{-1}$
P_{CO}	partial pressure of labelled CO, Pa
$P_{CO,tot}$	total pressure of CO, Pa
q	volumetric flow rate through the reactor cell, m^3 s^{-1}
R	gas constant, 8.314 Pa m^3 mol^{-1} K^{-1}
r_a	adsorption rate of labelled CO, mol m^{-3} s^{-1}
$r_{a,tot}$	total adsorption rate of CO, mol m^{-3} s^{-1}
r_d	desorption rate of labelled CO, mol m^{-3} s^{-1}
$r_{d,tot}$	total desorption rate of CO, mol m^{-3} s^{-1}
t	time, s
T	temperature, K
V	volume of reactor cell, m^3
x	length coordinate perpendicular to the external disc surface, m

Greek Symbols

ε	void fraction
θ	fractional coverage of labelled CO
$\theta_{CO,tot}$	total fractional coverage of CO
μ	linear absorption coefficient for β^- particles, m^{-1}
ρ	density of catalyst disc, kg m^{-3}

ACKNOWLEDGMENT

The financial support of the Swedish Research Council for Engineering Sciences (TFR) is gratefully acknowledged.

REFERENCES

1. Campell, K. C., and Thomson, S. J., *Prog. Surf. Membr. Sci.* **9,** 163 (1975).
2. Berndt, G. F., *Catalysis* **6,** 144 (1983).
3. Thomson, S. J., in "Characterisation of Catalysts" (J. M. Thomas and R. M. Lambert, Eds.), p. 214. Wiley, Chichester, 1980.
4. Klier, K., Zettlemoyer, A. C., and Leidheiser, H., Jr., *J. Chem. Phys.* **52,** 589 (1970).
5. Malakhov, V. F., Shmachkov, V. A., Kollchin, A. M., Stepanov, B. E., and Tapilin, V. M., *in* "Vtoraya Vsesoyuznaya Konferentziya po Kinetike Kataliticheskikh Reaktzii," Vol. 2, p. 128. Novosibirsk, 1975; see also Zhdanov, V. P., and Zamaraev, K. I., *Catal. Rev.–Sci. Eng.* **24,** 373 (1982).
6. Yates, J. T., Jr., Duncan, T. M., Worley, S. D., and Vaughan, R. W., *J. Chem. Phys.* **70,** 1219 (1979).
7. Yates, J. T., Jr., Duncan, T. M., and Vaughan, R. W., *J. Chem. Phys.* **71,** 3908 (1979).
8. Yates, J. T., Jr., and Goodman, D. W., *J. Chem. Phys.* **73,** 5371 (1980).
9. Matsushima, T., *Surf. Sci.* **79,** 63 (1979).
10. Matsushima, T., *Surf. Sci.* **87,** 665 (1979).
11. Matsushima, T., *J. Catal.* **64,** 38 (1980).
12. Yamada, T., Onishi, T., and Tamaru, K., *Surf. Sci.* **133,** 533 (1983).
13. Yamada, T., and Tamaru, K., *Surf. Sci.* **146,** 341 (1984).
14. Yamada, T., and Tamaru, K., *Surf. Sci.* **138,** L155 (1984).

15. Tamaru, K., and Yamada, K., *Shokubai* **27,** 350 (1985).
16. Yamada, T., and Tamaru, K., *Z. Phys. Chem. N.F.* **144,** 195 (1985).
17. Tamaru, K., Yamada, T., Zhai, R., Iwasawa, Y., *in* "Proceedings, 9th International Congress on Catalysis, Calgary, 1988" (M. J. Phillips and M. Ternan, Eds.), p. 1006. The Chemical Institute of Canada, Ottawa, 1988.
18. Tamaru, K., *Colloids Surf.* **38,** 125 (1989).
19. Yamada, T., Iwasawa, Y., and Tamaru, K., *Surf. Sci.* **223,** 527 (1989).
20. Yamada, T., Zhai, R., Iwasawa, Y., and Tamaru, K., *Bull. Chem. Soc. Jpn.* **62,** 2387 (1989).
21. Zhdanov, V. P., *Surf. Sci.* **157,** L384 (1985).
22. Yamada, T., Onishi, T., and Tamaru, K., *Surf. Sci.* **157,** L389 (1985).
23. Zhdanov, V. P., *Surf. Sci.* **172,** L533 (1986).
24. Lombardo, S. J., and Bell, A. T., *Surf. Sci.* **245,** 213 (1991).
25. Guo, X., Song, Z., Zhang, L., Xiang, N., and Zhai, R., *Catal. Lett.* **12,** 7 (1992).
26. Shen, S., Zaera, F., Fischer, D. A., and Gland, J. L., *J. Chem. Phys.* **89,** 590 (1988).
27. Gland, J. L., Shen, S., Zaera, F., and Fischer, D. A., *J. Vac. Sci. Technol. A* **6,** 2426 (1988).
28. Parker, D. H., Fischer, D. A., Colbert, J., and Koel, B. E., *Surf. Sci. Lett.* **236,** L372 (1990).
29. Gland, J. L., Fischer, D. A., Shen, S., and Zaera, F., *J. Am. Chem. Soc.* **112,** 5695 (1990).
30. Gland, J. L., Fischer, D. A., Parker, D. H., and Shen, S., *Langmuir* **7,** 2574 (1991).
31. Parker, D. H., Fischer, D. A., Colbert, J., and Koel, B. E., *Surf. Sci.* **258,** 75 (1991).
32. Cider, L., and Schöön, N.-H., *Appl. Catal.* **68,** 191 (1991).
33. Cider, L., and Schöön, N.-H., *Appl. Catal.* **68,** 207 (1991).
34. Cider, L., and Schöön, N.-H., *Ind. Eng. Chem. Res.* **30,** 1437 (1991).
35. Cider, L., Schröder, U., Schöön, N.-H., and Albinsson, B., *J. Mol. Catal.* **67,** 323 (1991).
36. Schröder, U., Cider, L., and Schöön, N.-H., *in* "Studies in Surface Science and Catalysis" (L. Guczi, F. Solymosi, and P. Tétényi, Eds.), Vol. 75, p. 643. Elsevier, Amsterdam, 1993.
37. Hicks, R. F., Kellner, C. S., Savatsky, B. J., Hecker, W. C., and Bell, A. T., *J. Catal.* **71,** 216 (1981).
38. Peri, J. B., *in* "Catalysis—Science and Technology," (J. R. Anderson and M. Boudart, Eds.), Vol. 5, p. 171. Springer-Verlag, New York, 1984.
39. Wicke, E., and Kallenbach, R., *Kolloid Z.* **97,** 135 (1941).
40. Fuller, E. N., Schettler, P. D., and Giddings, J. C., *Ind. Eng. Chem.* **58,** 19 (1966); see also Skelland, A. H. P., "Diffusional Mass Transfer," p. 168. Wiley, New York, 1974.
41. Guo, X., and Yates, J. T., Jr., *J. Chem. Phys.* **90,** 6761 (1989).
42. Foger, K., and Anderson, J. R., *Appl. Surf. Sci.* **2,** 335 (1979).
43. Herz, R. K., Kiela, J. B., and Samuel, P. M., *J. Catal.* **73,** 66 (1982).
44. Ertl, G., *in* "Catalysis—Science and Technology" (J. R. Anderson and M. Boudart, Eds.), Vol. 4, p. 209. Springer-Verlag, New York, 1983.